

# Effect of Camber and Angles of Attack on Airfoil Characteristics

Rajat Rajnish<sup>1</sup>, N.S. Thakur<sup>2</sup>, Priyanshu Kumar Pant<sup>3</sup>

<sup>1 2 3</sup>National Institute of Technology Hamirpur

<sup>1</sup>PG Scholar, Center for Energy Studies, N.I.T Hamirpur, Himachal Pradesh, India

<sup>2</sup>Professor, Center for Energy Studies, N.I.T Hamirpur, Himachal Pradesh, India

<sup>3</sup>PG Scholar, Dept. of Mathematics and Scientific Computing, N.I.T Hamirpur, Himachal Pradesh, India

\*\*\*

**Abstract** -Research is underway to enhance the aerodynamic efficiency of air vehicles, wind turbines, and automobiles through diverse approaches. This study employs a comprehensive analysis of three criteria that define the shape, including the camber, position of the camber, and angle of attack of the airfoil. The objective is to unveil the overall design space. This study throws light on the relation and impact of airfoil parameters on airfoil characteristics. This research shows the fully coupled impact of camber, position of camber, and angle of attack on lift coefficient and drag coefficient. These results show the efficiency and performance of airfoils with varying chosen parameters and show the optimized airfoils in the region of study.

**Keywords:** Airfoil, Computational fluid dynamics, Efficiency, Cl/Cd ratio, Aerodynamics performance

## 1.INTRODUCTION

Airfoil shape plays the most important role in the overall performance of aerodynamic bodies; a lot of great studies have been done to create specific airfoil shapes for the desired design condition. Different shapes of the airfoil are used according to the needs of industries for their applications like in helicopters, micro aerial vehicles[1], compressors, wind turbines, and many more areas. Airfoils have very essential characteristics that are lift, drag, and airfoil efficiency. These features specify how well an airfoil performs in the specific application for which it is used. Analyzing the characteristics of the airfoil and their relationship with each other will direct us to use the optimized airfoil for specific applications. Airfoils have been researched for various purposes for a long time for various industries like aircraft, renewable industry for wind energy production, compressors, and much more. Mostly airfoils are the key element used by these industries for their applications, which means a good-performing airfoil is needed. A lot of research has been done on airfoil parameters like shape, structure, etc. The work done on the optimization of airfoil shape for wind turbine application[2]. Work by M. Rasoul Triandaz[3] about the effect of airfoil shapes on power performance if VWAT is much appreciable, 126 airfoils were analyzed. A lot of research has been there on methods for the advancement of airfoil shape sat trailing edge [4], [5], [6]Solidity effect on the performance of variable-pitch

VAWT[7]. Study on surface modification on aerodynamic characteristics of airfoil DU 06 W 200 [8]. About 20 airfoils were examined for the performance of an H-rotor Darrieus turbine by MH Mohammad[9]. Research Development and Testing of an Unconventional Morphing Wing Concept with Variable Chord and Camber[10], [11], [12], airfoil thickness effect on dynamic stall characteristics of High-Solidity Vertical Axis Wind Turbines. Researchers have innovated camber morphing mechanisms employing smart materials[13], [14]. These mechanisms enable the adaptive adjustment of airfoil curvature, enhancing aerodynamic efficiency and performance in various applications, including aerospace and wind energy. Mostly the area of attention is on the performance of airfoils in various applications, optimization methods for obtaining good-performing airfoils, and morphing techniques for airfoils. No doubt a large number of airfoils is being analyzed but mostly symmetrical and just by varying thickness and taking other effective parameters as constant. There is very little attention given to the dependency of parameters on each other and their relationship with the characteristics of airfoils. The research gap comes out of the studied literature on the analysis of asymmetric airfoils with varying camber, varying position of camber, and varying angle of attack (AoA) by establishing co-relation between them which will show the performance of airfoil and dependency of parameters on each other. This study aims to shed light on how structural characteristics affect the aerodynamic performance of asymmetrical airfoils. 16 NACA four digits modified asymmetric airfoils are analyzed by varying camber angles and their position concerning chord length(C), range shown in Table 1. The characteristics, lift and drag coefficient along with the Cl/Cd ratio are analyzed and co-relations are shown between these characteristics. This analysis is performed at Reynolds No. (Re)  $6.84 \times 10^5$  and velocity  $V=10$  m/s. The fluid used in CFD simulation is air having a density of  $1.225$  kg/m<sup>3</sup>. Varying the camber and its position provide major aerodynamic advantages by allowing for unique and large shape modifications to accommodate varied flight situations, in turbines for efficient power generation, and many other applications where airfoils are used for specific purposes to enhance the performances. These analyses show changes in airfoil efficiency and relations of airfoil characteristics with each other. Notably, the drag and lift coefficient parameters (Cd) and (Cl)are critical,

making morphing wings a viable strategy for improving airfoil performance. The thickness ( $t = 24\%C$ ), leading-edge radius index ( $I = 4\%C$ ), and position of a thickness ( $x_t = 30\%C$ ) are taken constant.

### 1.1 NACA 4-Digit Airfoil

The NATIONAL ADVISORY COMMITTEE FOR AERONAUTICS (NACA) produced NACA airfoils, which are airfoil forms for aircraft wings. A series of numerals following the term NACA describes the shape of the NACA airfoils. The NACA Four-Digit Series was the first family of airfoils to be constructed with this method. The maximum camber ( $M$ ) in the percentage of the chord (airfoil length) is specified by the first digit, the maximum camber position ( $P$ ) in tenths of the chord is indicated by the second, and the maximum thickness ( $t$ ) of the airfoil in the percentage of the chord is given by the final two digits. For example, the NACA 2415 airfoil has a maximum thickness of 15% with a camber of 2% positioned 40% back from the airfoil leading edge (or  $0.4c$ ). With these  $m$ ,  $p$ , and  $t$  values, we can use the following relationships to get the coordinates of an airfoil [15]

$$y_c = \frac{M}{P} * (2Px - x^2)x^2 \quad (0 \leq x < P)$$

$$y_c = M / (1-P) * (1-2P + 2Px - x^2) \quad (P \leq x \leq 1)$$

The modified airfoil profile coordinates are generated with the help of Open VSP software. This helps us to plot 2-D modified airfoils with various camber and position changes.

### 1.2 Naming Scheme of NACA 4-Digit Modified Airfoil

The airfoil will be identified with the name NACA MPt-Ixt where  $I$  is the leading edge radius index and  $x_t$  will show the position of maximum thickness of the airfoil. All the parameter locations are shown in Fig.1.

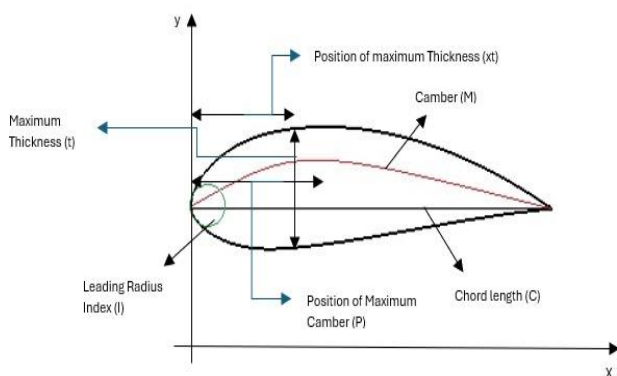


Fig -1: Shape parameter of asymmetric airfoil

Table -1: Range of analyzed parameters in percentage (%)  
Chord length (C) = 1 meter

Parameters		
Camber (M)	Position of camber (P)	The angle of Attack (AoA in degree)
2	20	0
3	30	5
4	40	10
5	50	15

## 2. Design and Meshing

NACA MPt-Ixt airfoils are designed in Open VSP software. The number of airfoils analyzed is 16 having different parameters varying the camber and camber's location. The chord length of the airfoil is 1 meter, and the Leading-edge radius index ( $I$ ) is 4% of  $C$ . The thickness is constant i.e. 24% of  $C$  and the position of thickness is taken at 30% of  $C$ . The shape of all 16 profiles is shown in Fig.2. The semicircular and rectangular domain known as C type mesh domain is used having 200000 elements inside the mesh. The C type is better to use for 2-D surfaces as we can produce structured cells and uniform structures of cells near complex geometry. To accurately estimate flow near walls, particularly for airfoils with high-pressure gradients, the structured mesh is more frequently used around these intricate geometries. Moreover, it uses less memory and time than unstructured grids. The simulations were carried out in Ansys Fluent v2023R2. The type of mesh and domain is shown in Fig.3.Z

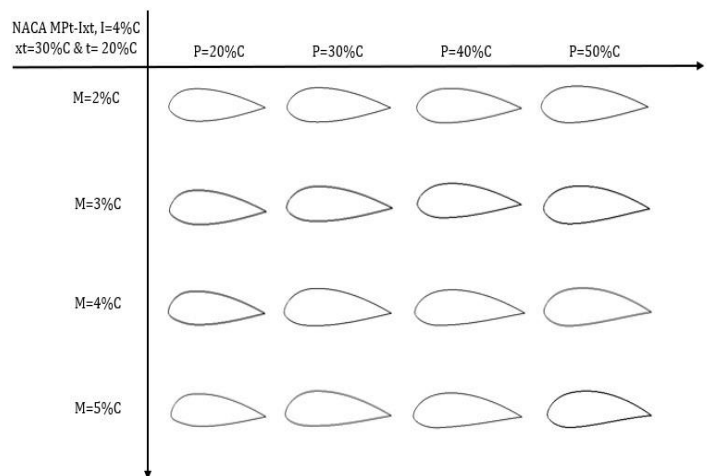


Fig -2: Analyzed Airfoil Profiles

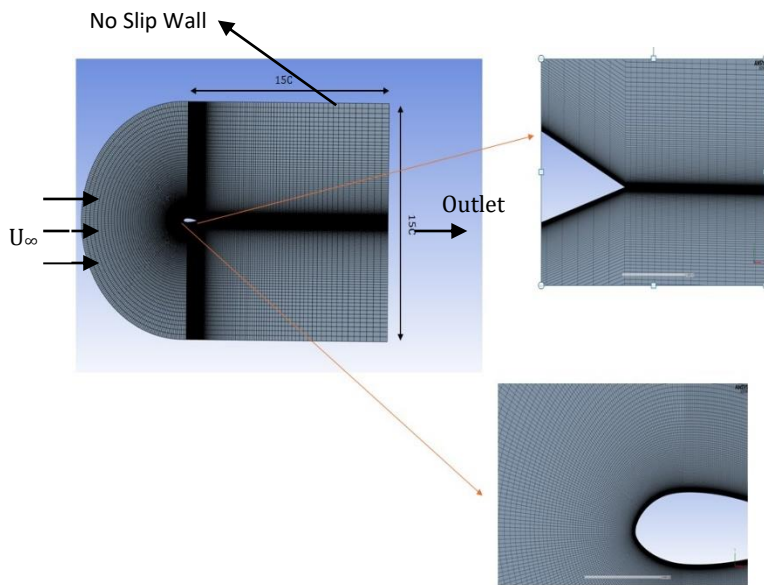


Fig -3: Schematic mesh and Domain of Airfoil

### 3. Computational Settings

The simulations are based on the URANS SST model. The turbulence model used in this study was chosen after a thorough critical examination of seven commonly used Reynolds-averaged eddy-viscosity turbulence models in three separate and diverse experimental setups. [66 refs, 15models]. We choose the Transition SST model because it gives the most accurate results with experimental results for NACA 2412 airfoil.[16] as shown in chart -1. The transition SST model combines the  $k-\epsilon$  model for the free stream and the  $k-\omega$  model for flow near walls. The inlet conditions used for turbulence are intermittent is 1, turbulence intensity is 5%, and turbulence viscosity ratio is 10. The outlet condition is set as a pressure outlet. The coupled scheme is used for pressure velocity coupling all with second-order spatial discretization. Several 1000 iterations were employed for better convergence of simulation results.

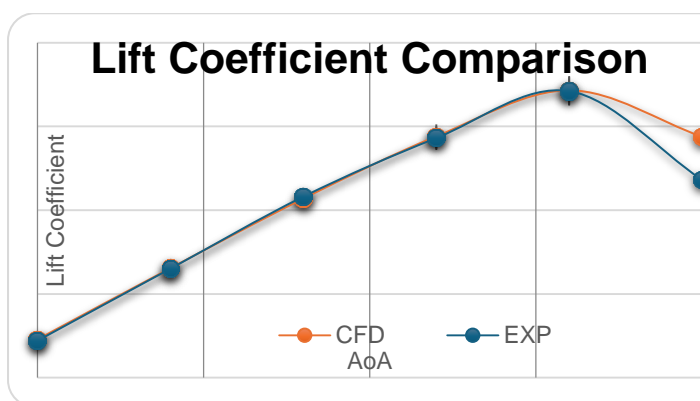
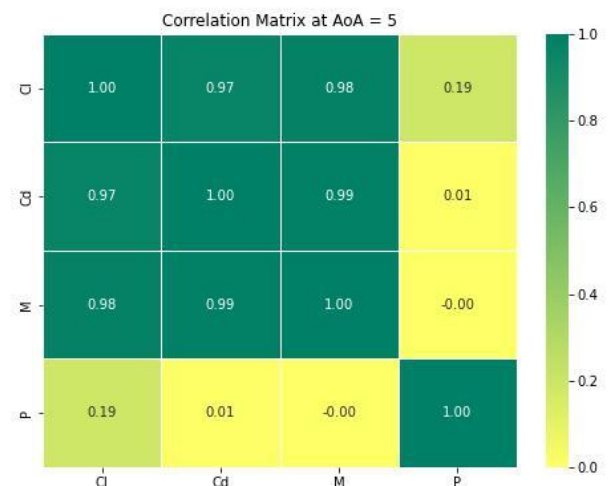
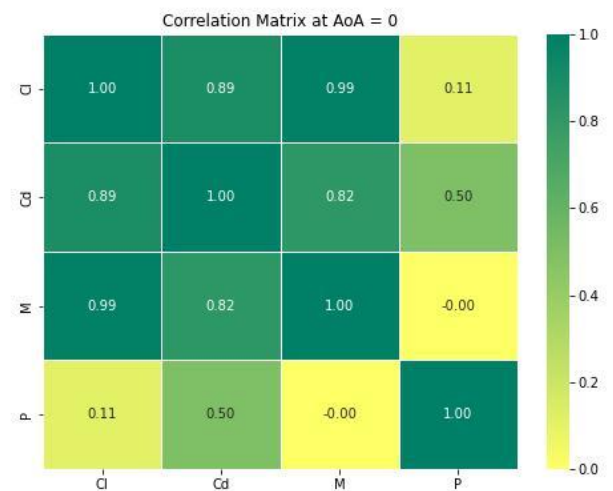


Chart -1: Cl comparison with CFD vs Experiment of NACA 2412

## 4. Results

### 4.1 Correlation Matrix at Different AoA.

A correlation matrix is important because it can reveal relationships, influence the selection of variables, and improve a general understanding of the dataset. The correlation matrix in Fig.4 shows the relation of  $C_l$ ,  $C_d$ ,  $M$ , and  $P_{at}$  different AoA with each other. Factor 1 shows the impact of the dependency is highest, factor 0 shows the impact of no dependency, and the negative factor shows the inverse dependency of the parameters with each other.



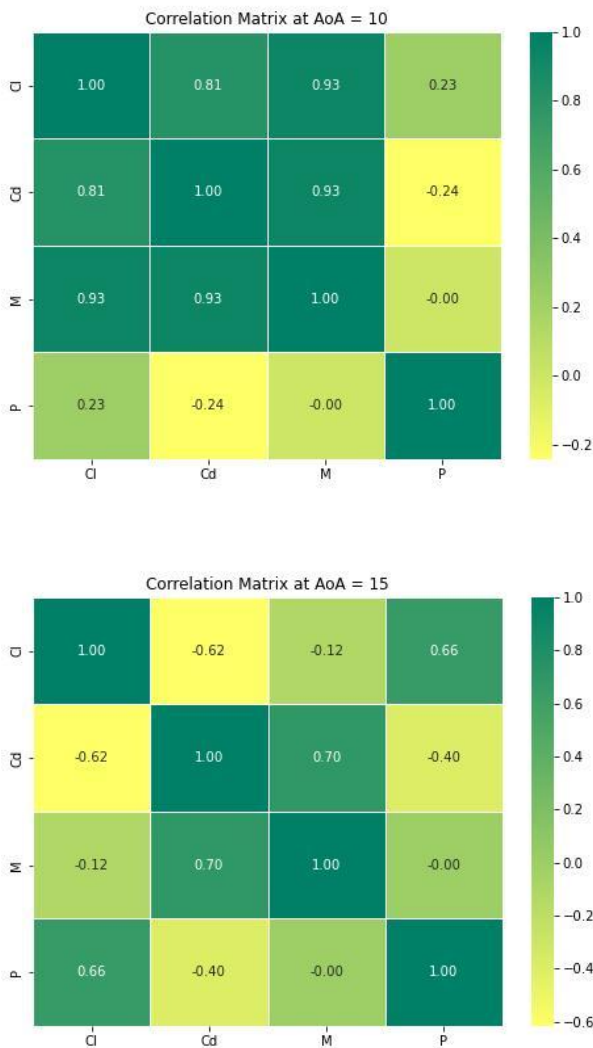


Fig -4: Correlation matrix at Different AoA.

**(a). Cl correlation with Cd, M, and P**

Cl has a correlation with Cd of 0.89 from AoA 0-10, which climbs to 0.97 at AoA 5 and subsequently decreases to -0.62 at AoA 15. This shows that Cl and Cd have a directly proportional relation till 10 degrees if Cl will increase then Cd will also increase. The correlation of Cl and Cd on each other has a high impact and after AoA 15 will inversely affect each other. The impact of the correlation of Cl with camber (M) at 0 degrees is highest at 0.99 but starts to decrease as we increase AoA. At 15 degrees Cl will have an inverse relation i.e. if we increase AoA then Cl will decrease if we increase the camber. The Cl relation with the camber (P) position increases as we increase AoA. At 0 degrees the impact of correlation of Cl with P is 0.11 which further increases to 0.66 at AoA 15 degrees. This shows the Cl will increase as we increase the position of the camber to 5% of C with increasing AoA value.

**(b).Cd correlation with P and M**

Cd has a correlation with M of 0.82 at AoA 0 degrees and 0.99 at 5 degrees then further it decreases to 0.70 at 15 degrees. The value of Cd is all positive with M as the relation is directly proportional with (M), but the impact of correlation decreases as we increase AoA from 5-15 degrees. The impact of the correlation of Cd with the position of camber (P) is highest at 0 degrees i.e. 0.50, but further decreases to 15 degrees which are -0.40. This shows that with an increase in the P to 50%C, the inverse relation starts at 10 degrees which means after 10 AoA if we further increase P will decrease the Cd.

**(c). P and M correlation**

The parameters P and M show the impact of 0 which means they do not establish any relation and do not have any relation with each other. This is because P and M are independent parameters that do not affect each other. They are values set by individuals to design the airfoil, but they both impact the characteristics such as Cl, Cd, and efficiency of the airfoil.

**4.2 Effect on Cl and Cd with varying M and P**

Fig 4a, 4e. Shows the effect of varying camber with AoA and keeping the position of camber constant. At P=20%C, the Cl of the airfoils increases till 10 degrees AoA, but profile 5224 has a sudden drop in Cl, and 3224 performs the best among the profiles in Fig 5a. The difference of Cl between 3224 and 5224 is 20.11% at 15 degrees. This shows that the Cd for 3224 is less than 5224 at a high angle of attack i.e. 15 degrees, the difference between Cd of 3224 and 5224 is 45.18%. Airfoil 2224 and 4224 have gradually increased in Cl to 15 degrees AoA. Both have almost the same Cl at 15 degrees with a difference of 1.73%. Fig 4b,4f shows at P=30%C the Cl of all the profiles increases up to 15 degrees AoA except profile 5324 whose Cl increases to 10 but decreases at AoA 15 degrees. Airfoil 4324 has the highest Cl and 2324 has the lowest Cl at AoA 15 degrees with a difference of 17.02 %. The airfoils 5324 and 3324 are almost at the same Cl at 15 degrees with almost a difference of 9%. Due to camber change the drag on airfoil 5324 is the highest. In Fig 4c, 4g at P=40%C, airfoils almost show the same behavior as in Fig 4a, 4e Cl difference between airfoil 3424 and 5424 is 16.82. In Fig 4d, 4h at P=50%C shows that there is a gradual increase in Cl and Cd of all profiles and very little difference between Cl and Cd of airfoils. The Cl shows the converging behavior at AoA 15 degrees when we take P=50%C. These graphs show the effects of varying camber and position of camber on Cl and Cd, which helps identify the airfoil that can give good performance concerning conditions we need.

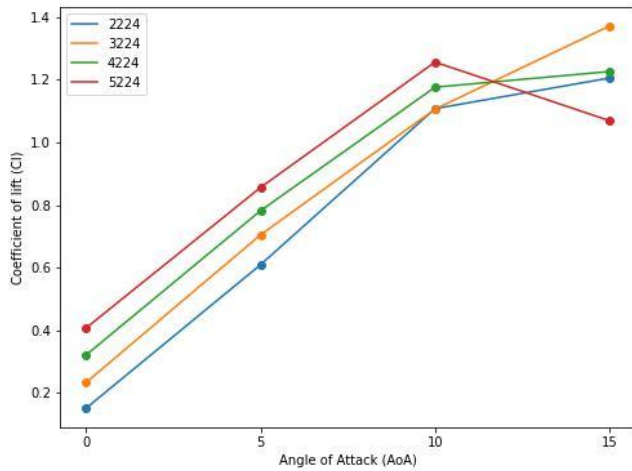


Fig -4a: Effect on Cl with varying camber at P=20%C

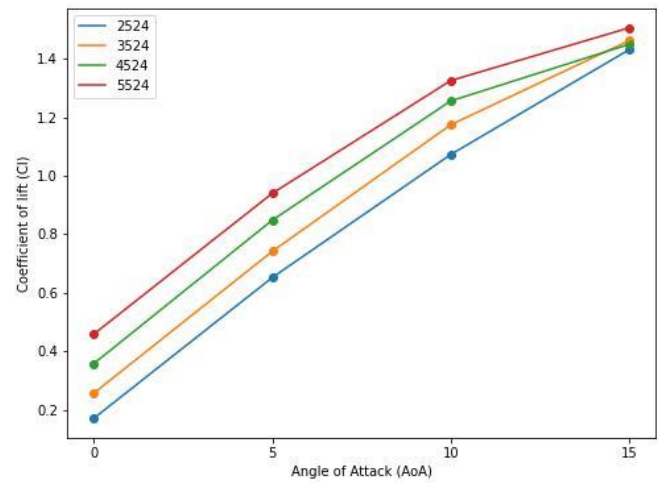


Fig -4d: Effect on Cl with varying camber at P=50%C

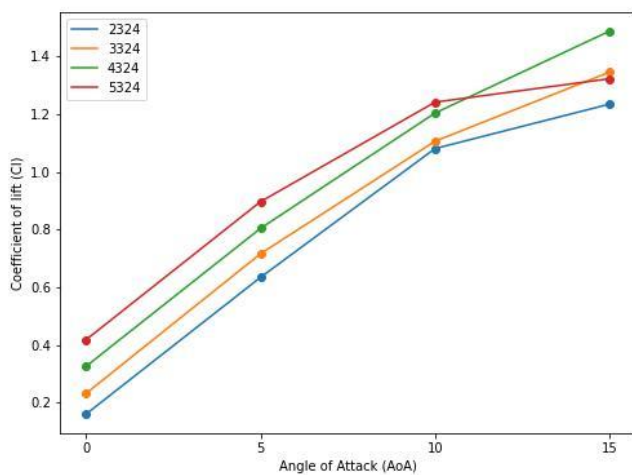


Fig -4b: Effect on Cl with varying camber at P=30%C

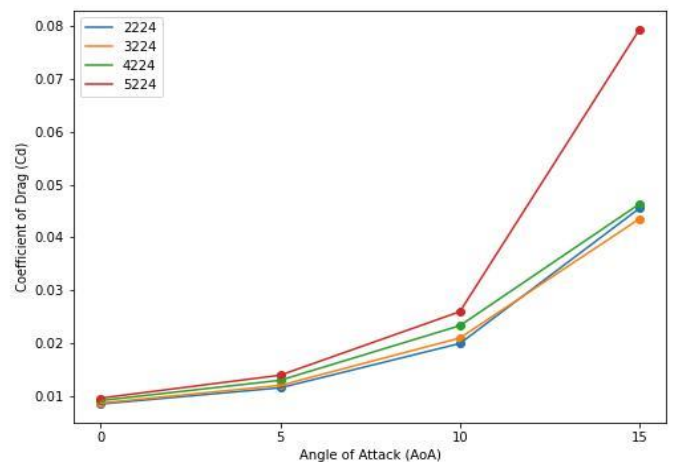


Fig -4e: Effect on Cd with varying camber at P=20%C

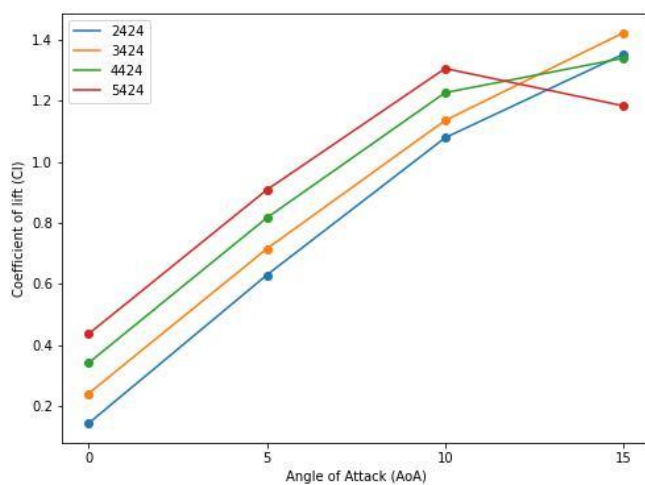


Fig -4c: Effect on Cl with varying camber at P=40%C

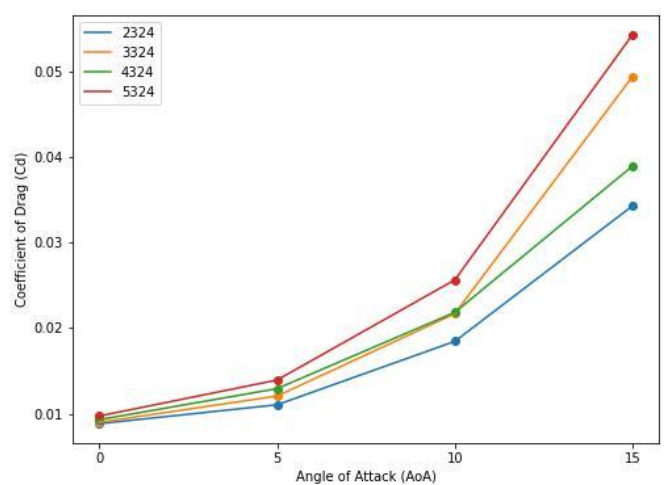


Fig -4f: Effect on Cd with varying camber at P=30%C

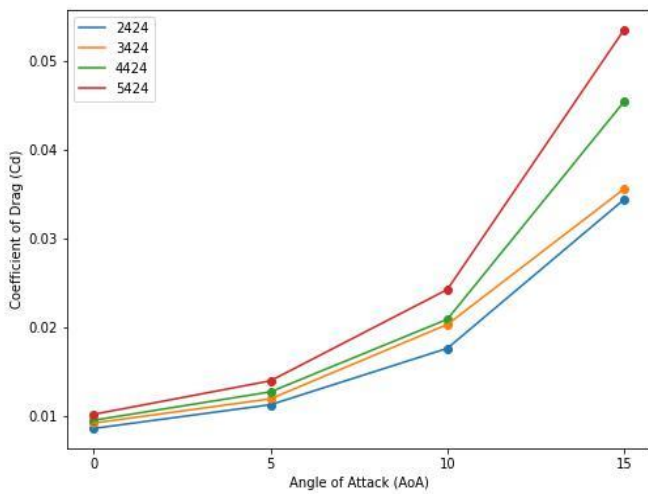


Fig -4g: Effect on Cd with varying camber at P=40%C

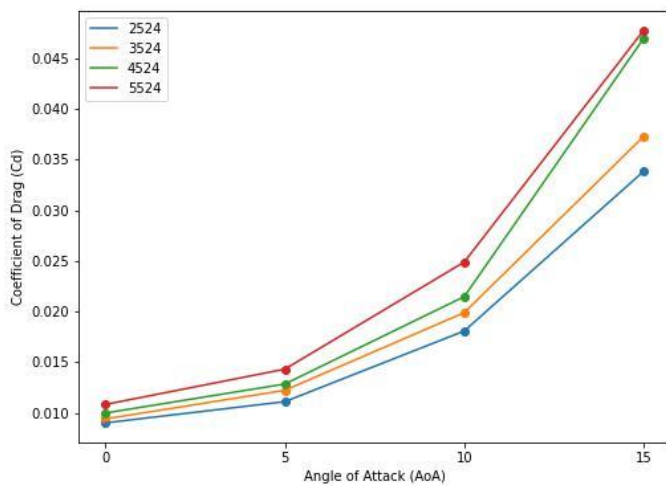


Fig -4h: Effect on Cd with varying camber at P=50%C

### 4.3 Impact of AoA on Cl and Cd of Airfoils

Fig 5 depicts that the Cd of the airfoils increases gradually and with almost some consistency with change in AoA till 10 degrees, but for AoA 15 degrees the sudden increases and decreases in Cd the pattern not consistent which is due to the generation of the wake region which gives rise to stall conditions due to these stall conditions the lift starts to decrease at high angles of attacks. The Cd for 5224 is the highest at AoA 15 degrees and the Cl is low for this at AoA 15 degrees. There is an increase of almost 20% in Cl from airfoil 2224-5524 at 15 degrees, 16.47% at 10 degrees, 35.21% at 5 degrees, and 67.11% at) degrees AoA

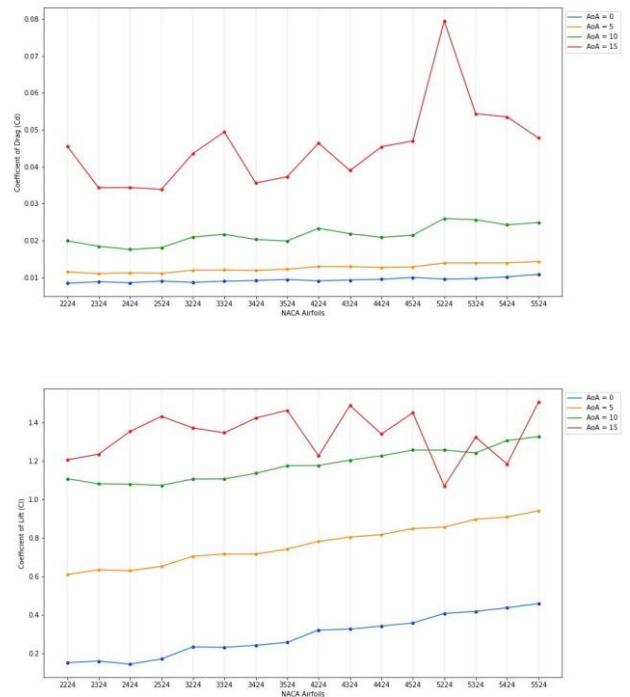


Fig -5: Effect on Cd with varying camber at P=50%C

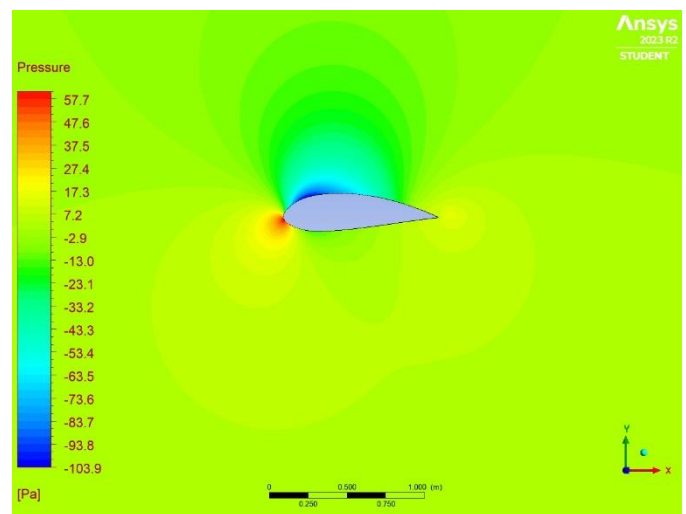


Fig -5a: Pressure Contour of airfoil 4524 at 5 degrees AOA

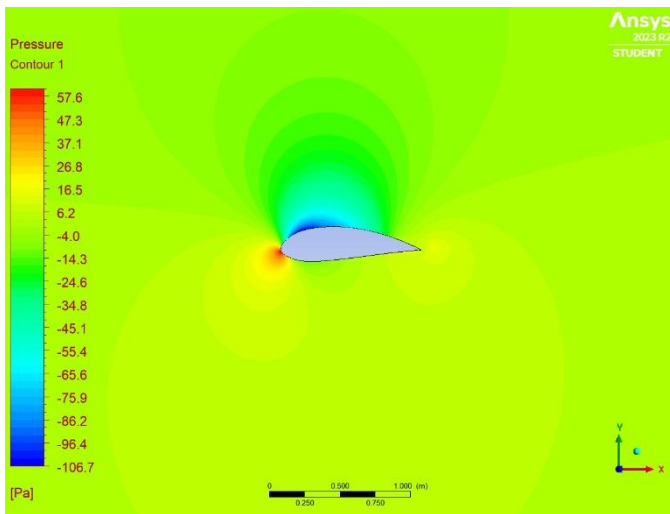


Fig -5b: Pressure Contour of airfoil 5524 at 5 degrees AOA

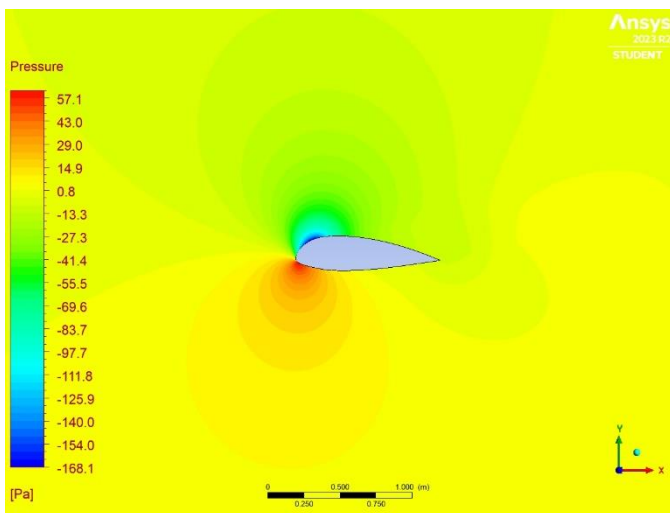


Fig -5c: Pressure Contour of airfoil 5224 at 15 degrees AOA

#### 4.4 Efficiency of Airfoils

Efficiency is defined by L/D ratio or Cl/Cd ratio. The higher the ratio more efficient will be the airfoil in the aspect of performance, which means the airfoil has the high lift and least drag which is the most required condition of airfoil. Airfoil 4524 at AoA 5 degrees has the highest Cl/Cd ratio i.e. 65.98 and Airfoil 5524 at AoA 5 degrees has a value of 65.65 which is very close to airfoil 4524's ratio. Airfoil 5224 has the least ratio i.e. 13.46.

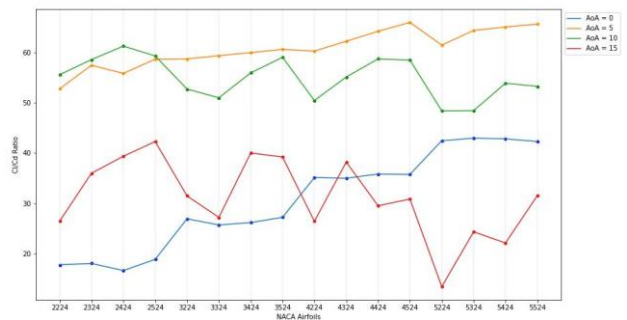


Fig -7: Cl/Cd of Airfoils

## 5. CONCLUSIONS

Within this study range the conclusions are as follows:

- From the correlation matrix it says that there is a relation between Cl and Cd which is directly proportional up to AoA 10 degrees and inversely proportional after 10 degrees.
- The Cl decreases if we only change the camber (M) and take other parameters constant, but Cl increases when we change the position of the camber (P).
- P and M are independent of each other and do not impact each other.
- The Cl increases gradually for all airfoils up to 15 degrees, but the airfoil of camber 5% C Cl decreases after 10 degrees except for the 5524 airfoils. The Cd for all airfoils increases as we increase M and P.
- Airfoil 5524 has the highest Cl among studied airfoils at 15 degrees AoA and airfoil 2224 has the least Cl.
- Two airfoils 4524 and 5524 are the most efficient in the studied region having Cl/Cd ratios of 65.98 and 65.65 respectively. Airfoil 5224 has the lowest Cl/Cd ratio of 13.46.

Finally, the study emphasizes how the two shape-defining parameters of asymmetric airfoils interact to affect their efficiency and characteristics. It underlines that isolating one parameter while leaving others constant can lead to inconclusive results. The study shows that changing the parameters leads to changes in characteristics and efficiency. The correlation matrix study also shows there is also the relation of characteristics and parameters with each other which shows the behavior of characteristics with each other.

## REFERENCES

- [1] N. S. K. Teja, A. Teja, J. S. Harsha, S. Ganesh, and K. V Ramana, "OPTIMIZATION OF MICRO AIR VEHICLE AIRFOIL." [Online]. Available: <http://www.irjet.org>
- [2] A. F. P. Ribeiro, A. M. Awruch, and H. M. Gomes, "An airfoil optimization technique for wind turbines," *Appl Math Model*, vol. 36, no. 10, pp. 4898–4907, Oct. 2012, doi: 10.1016/j.apm.2011.12.026.
- [3] M. R. Tirandaz and A. Rezaeiha, "Effect of airfoil shape on power performance of vertical axis wind turbines in dynamic stall: Symmetric Airfoils," *Renew Energy*, vol. 173, pp. 422–441, Aug. 2021, doi: 10.1016/J.RENENE.2021.03.142.
- [4] P. L. Bishay *et al.*, "Development of an SMA-based camber morphing UAV tail core design," *Smart Mater Struct*, vol. 28, no. 7, p. 075024, Jul. 2019, doi: 10.1088/1361-665X/ab1143.
- [5] H. Li, L. Liu, T. Xiao, and H. Ang, "Design and simulative experiment of an innovative trailing edge morphing mechanism driven by artificial muscles embedded in skin," *Smart Mater Struct*, vol. 25, no. 9, p. 095004, Sep. 2016, doi: 10.1088/0964-1726/25/9/095004.
- [6] L. Hongpeng, W. Yu, Y. Rujing, X. Peng, and W. Qing, "Influence of the modification of asymmetric trailing-edge thickness on the aerodynamic performance of a wind turbine airfoil," *Renew Energy*, vol. 147, pp. 1623–1631, Mar. 2020, doi: 10.1016/J.RENENE.2019.09.073.
- [7] M. T. Parra-Santos, C. N. Uzarraga, A. Gallegos, and F. Castro, "Influence of Solidity on Vertical Axis Wind Turbines," *International Journal of Applied Mathematics, Electronics and Computers*, vol. 3, no. 3, p. 215, Jun. 2015, doi: 10.18100/IJAMEC.42848.
- [8] O. A. Zargar *et al.*, "The effects of surface modification on aerodynamic characteristics of airfoil DU 06 W 200 at low Reynolds numbers," *International Journal of Thermofluids*, vol. 16, p. 100208, Nov. 2022, doi: 10.1016/J.IJFT.2022.100208.
- [9] M. H. Mohamed, "Performance investigation of H-rotor Darrieus turbine with new airfoil shapes," *Energy*, vol. 47, no. 1, pp. 522–530, Nov. 2012, doi: 10.1016/j.energy.2012.08.044.
- [10] W. R. Kang, E. H. Kim, M. S. Jeong, I. Lee, and S. M. Ahn, "Morphing wing mechanism using an SMA wire actuator," *International Journal of Aeronautical and Space Sciences*, vol. 13, no. 1, pp. 58–63, 2012, doi: 10.5139/IJASS.2012.13.1.58.
- [11] T. Majid and B. W. Jo, "Comparative Aerodynamic Performance Analysis of Camber Morphing and Conventional Airfoils," *Applied Sciences*, vol. 11, no. 22, p. 10663, Nov. 2021, doi: 10.3390/app112210663.
- [12] J. Zhang *et al.*, "Aeroelastic model and analysis of an active camber morphing wing," *Aerosp Sci Technol*, vol. 111, p. 106534, Apr. 2021, doi: 10.1016/J.AST.2021.106534.
- [13] H. Basaeri, A. Yousefi-Koma, M. R. Zakerzadeh, and S. S. Mohtasebi, "Experimental study of a bio-inspired robotic morphing wing mechanism actuated by shape memory alloy wires," *Mechatronics*, vol. 24, no. 8, pp. 1231–1241, Dec. 2014, doi: 10.1016/j.mechatronics.2014.10.010.
- [14] D.; Keidel, J.; Sodja, N.; Werter, R.; De Breuker, and P. Ermanni, "Development and Testing of an Unconventional Morphing Wing Concept with Variable Chord and Camber," APA, 2015.
- [15] "A-1 Appendix A Geometry for Aerodynamicists."
- [16] H. Abbott and Albert E. Von, *Theory of Wing Sections - Ira H. Abbott and Albert E. VonDoenhoff*.